https://doi.org/10.1016/j.jpowsour.2015.05.025

Enhanced Efficiencies in Thin and Semi-Transparent Dye-Sensitized Solar Cells under Low Photon Flux Conditions Using TiO_2 Nanotube Photonic Crystal

Keyu Xie[a, b], Min Guo[b], Xiaolin Liu[b], Haitao Huang[b,*]

[a] *State Key Laboratory of Solidification Processing and Center for Nano Energy Materials, Northwestern Polytechnical University, Xi'an, 710072, China*

[b] *Department of Applied Physics and Materials Research Centre, The Hong Kong Polytechnic University, Hong Kong, China*

* Corresponding author.

Tel: +852-2766-5694; E-mail: aphhuang@polyu.edu.hk

Abstract: The photovoltaic output of dye-sensitized solar cells (DSSCs) are greatly dependent on the amount of absorbed photons, which is limited by the thickness of active layer of DSSCs and the illumination conditions. To improve the cell performance under low irradiance condition, a photoanode was designed by attaching a TiO_2 nanotube photonic crystal (NTPC) onto the thin TiO_2 nanoparticle (NP) layer

for applications in thin and semi-transparent DSSCs. It is found that the introduction of the TiO_2 NTPC significantly increases the light harvesting and hence the power conversion efficiency (PCE) of the respective DSSCs. The TiO_2 NTPC provides multi-functionalities, such as Bragg reflection, light scatting and additional light harvesting from its nanotube structure, leading to more significant light harvesting enhancement in these thin and semi-transparent DSSCs. Compared with the single-layer TiO_2 NP based reference DSSCs, the above-mentioned synergic effects in a cell incoporated with a ~2.3-μm-thick TiO_2 NTPC yield PCE enhancements up to 99.1% and 130%, respectively, under 1 and 0.5 Sun conditions, respectivly. Meanwhile, an obvious compensation effect of TiO_2 NTPC to reduce the output power drop of these cells under tilted incient light is also demonstrated. The work will boost the practical applications of PC in irradiance sensitive devices.

Keywords: TiO_2 Nanotube Photonic Crystal; Photoanode; Low Photon Flux Condition; Thin and Semi-Transparent Dye-Sensitized Solar Cells.

Highlights:

1. A thin and semi-transparent TiO_2 NTPC/NP photoanode is proposed.
2. The anodic TiO_2 NTPC provides multi-functionalities to enhance the PCE of DSSC.
3. With the NTPC, the PV properties under low photon flux conditions were improved.

1. Introduction

Dye-sensitized solar cells (DSSCs) have attracted a great deal of attention due to their low-cost, simple fabrication process, as well as some other attractive properties, such as vivid color, transparency, and acceptable response at low irradiance or diffuse radiation conditions[1,2]. Efficiencies up to 13% have been achieved on a laboratory scale[3]. Nevertheless, almost all of the DSSCs with high performances require the use of an additional diffuse scattering layer, which is made of larger particles to reflect light back in random directions, onto a thick nanoparticle (15-20nm) crystalline TiO_2 (nc-TiO_2) absorbing layer[3-5]. The diffuse scattering layer prevents the devices from being transparent and color-tunable. Removing this scatter layer is definitely beneficial to the transparency of DSSCs, but it also reduces the amount of absorbed photons, and thus the power conversion efficiency (PCE) of DSSCs at the same time. Hence, how to achieve a high-efficiency of DSSC while keeping its transparency and tunable color is a challenge.

Fortunately, in order to further improve the PCE and stability of cells for real commercial applications, much progress has been made in searching for new dye-sensitizers, such as porphyrin-based dyes and polythiophene containing dyes[3,6-8], as well as alternative electrolyte to the iodide-based liquid one, such as Co(II)/Co(III) redox mediator[3,9] and solid-state hole transporting materials (HTMs)[10,11]. These strategies make thin and transparent DSSCs with high-efficiency possible. For example, the introduction of new dye-sensitizer with higher molecular extinction coefficient allows the reduction of the thickness of the

TiO_2 nanoparticle active layer without comprising the photocurrent of the device. Moreover, the new cobalt complex redox, which helps to increase the open circuit voltage (V_{oc}) of DSSCs over 1000mV, also requires a thinner nc-TiO_2 film because of its short electron lifetime[9]. As for the HTMs, which is used in the solid-state DSSCs (ss-DSSCs) to offer both high voltage output and long-term stability, the poor pore filling fraction and short diffusion length of charge carriers[12,13] limit the thickness of nc-TiO_2 film to be around 2~3μm, nearly 1/5 the thickness in a liquid cell. Hence, new strategies and concepts are urgently needed to achieve a high efficiency of the DSSC equipped with a thin-electrode.

Apart from the thickness limitation, insufficient light irradiation should also be taken into consideration for practical applications of DSSCs, such as in the case of decorative architectural glass which is normally installed away from the optimum orientation and in the situation where a light tracking system is hardly applied[14,15]. In order to achieve widely applications of DSSCs in consumer electronics, an attractive market for DSSCs[16], the cells should be able to maintain reasonable efficiencies under low irradiance, such as room light illumination.

Since Mallouk's first use of inverse opal structure in DSSCs to enhance the light harvesting efficiency in 2003, photonic crystal with selective spectral response has attracted considerable interest as an effective photon management method for solar cells[17-19]. More and more new concepts and structures are emerging for better control of light propagation in the cells without interfering the charge transport and collection processes. For example, porous 1D photonic crystal with increased porosity

has been proposed to allow electrolyte diffusion in the electrode facilely[20,21]. In addition, a novel TiO_2 nanotube photonic crystal (NTPC) has recently been fabricated and employed in thick-electrode DSSCs to increase the PCE (η) by 39.5%[22,23].

In order to conquer the challenges met in practical applications of thin-electrode DSSCs and to obtain high photocurrent efficiency under reduced irradiance, a hierarchical photoanode consisting of the newly designed TiO_2 NTPC with optimized lattice constant and a thin TiO_2 nanoparticle layer is proposed in the present study. The TiO_2 NTPC provides photon management through Bragg reflection and scattering effect. The anchoring of dye on the surface of TiO_2 nanotubes makes additional contribution to light harvesting, leading to a significant increase in PCE. It is found that the efficiency enhancement due to the embedded TiO_2 NTPC shows an increasing trend as the thickness of the NP layer is decreasing, yielding a PCE of 4.66% for ~2.3-μm-thick TiO_2 NTPC coupled thin-electrode (3μm NP layer) DSSCs at the incident irradiation intensity of 100mW·cm^{-2}. The η is further increased to 5.03% in low illumination intensity of 50mW·cm^{-2}, which is 130% higher than that of the reference DSSC which is solely based on NP photoanode. Meanwhile, a slower drop of photocurrent efficiency with increasing incident angle is also observed in thin and semi-transparent DSSCs equipped with the TiO_2 NTPC as compared with the reference cells.

2. Experimental

2.1 Materials

Titanium foils (99.7%, 0.125mm thick) were purchased from Strem Chemical (USA). Ammonium fluoride (96%), Ethylene glycol (EG, 99.5%), acetone and ethanol were purchased from International Laboratory (USA). Ruthenium dye (535-bisTBA, N719), TiO_2colloidal NP paste (13nm), FTO conducting glass (Transmittance of visible light⩾90%, 14 ohms/sq, 2.2μm thick), Pt-coated FTO glass, and the electrolyte (DMPD: 1.0 M, LiI: 0.1 M, 4-TBP: 0.5 M, I2: 0.12 M, 3-methoxy propionitrile) were purchased from Wuhan Geao Instruments Science and Technology Co. Ltd (China). Deionized (DI) water (18.2 MΩ) was obtained with Direct-Q3 Water Purification Systems made by Millipore Corporation. All solvents and chemical reagents used in our experiments were obtained from commercial sources as guaranteed reagent grades and used without further purification.

2.2 Synthesis of TiO_2 NTPC

Potentiostatic anodization of Ti foils was performed at 60V for 15min in EG solution containing 0.5 wt% ammonium fluoride and 3 vol% DI water using a platinum cathode. Then the developed TiO_2 NT array was peeled off by ultrasonic treatment in DI water for 5-10min to get flat Ti surface. A second anodization was conducted to produce TiO_2 NTPCs, using periodic alternating high current (so determined to obtain an anodization voltage of ~60V) and low current (0A) pulses, as described in previous work[22,23]. The high and low current pulse durations were set as 30 and 90s, respectively, to obtain TiO_2 NTPCs with a lattice constant of ~150nm, which have been shown to have the best matched bandgap with the absorption range of N719 under normal illumination. Different pulse numbers were used to adjust the

periods of TiO_2 NTPCs (TiO_2 NTPC with 15, 30, 45 and 60 periods are named as 15c NTPC, 30c NTPC, 45c NTPC and 60c NTPC, respectively, and the corresponding thicknesses of the TiO_2 NTPC membrane are about 2.3, 4.5, 6.7 and 9μm, respectively.

2.3 Fabrication of DSSCs

A freestanding TiO_2 NTPC film was detached from the Ti substrate by a subsequent potentiostatic anodization at 60V for 2h in the same EG solution, after a heat treatment at 270°C for 1h. The TiO_2 NTPC film was then transferred onto a TiO_2 NP paste coated FTO substrate, which was deposited by a doctor blade technique. After annealing at 450°C for 3h, good adhesion between the TiO_2 NTPC and the TiO_2 NP film with a thickness of about 3, 5 and 10μm was achieved. The integrated photoanodes were then immersed into 0.3mM N719 in ethanol for 24h at 60°C, followed by rinsing in pure ethanol. The sandwich type cell was assembled with the photoanode, Pt coated counter electrode and electrolyte, and sealed by a thermal adhesive film. For comparison, reference cells with only a TiO_2 NP layer of the same thickness were also prepared. For each type of DSSCs, 5-6 cells were fabricated and tested.

2.4 Characterization of photoanodes and solar cells

The morphology and architecture of the TiO_2 NTPC and photoanodes were observed with field emission scanning electron microscope (FESEM, JEOL JSM-6335F). The optical properties of the photoanodes were investigated by a UV-Vis spectrophotometer (Model UV-2550, Shimadzu, Japan), and the reflectance

spectrum were obtained using an integration sphere. I-V characteristics of DSSCs were measured by a Keithley 2400 source meter with a Newport 91160 solar-light simulator of an AM 1.5 filter. The active area of the working electrode was about 0.16 cm^2 with a black mask wrapping around the electrode and its lateral sides to avoid spurious light influence. In the I-V measurement, a rotational sample holder was used for angular measurements and the light intensity certified by a silicon reference solar cell was adjusted with a Newport 69911 power source. The incident photon-to-current efficiency (IPCE) was obtained by a Newport 2931-C power meter with the light source from a Newport 66902 solar simulator. The light intensity was measured with a Newport 2931-C power meter equipped with a 71675_71580 detector probe.

2.5 Simulation and theoretical calculation

Finite-element full wave simulation was employed for the numerical calculation of absorption spectra. The theoretical model of the photoanode, according to the experimental sample, consists of a TiO_2 NTPC slab and a TiO_2 NP layer of 50% porosity (effective refractive index=2.03) with the same thickness as the experimental sample. The TiO_2 NTPC was modelled with the nanotubes sitting in a hexagonal lattice, whose diameter and wall thickness were 110 and 10nm, respectively, and the refractive index was 2.51. In the model, the light first passed through the transparent glass with a refractive index of 1.45 and then reached the photoanode from the TiO_2 NP side. Finally, the electrolyte with a refractive index of 1.403, similar to that of propionitrile electrolyte, was modelled as the last layer. All the photoanodes, including TiO_2 NP and NTPC, were sensitized by ruthenium dye whose absorption

coefficient was obtained by fitting the photocurrent and the absorptance spectra of similar layer and device and was represented by the frequency-dependent imaginary part of the refractive index.

For the theoretical estimation of the photocurrent enhancement (ΔJ_{sc}), the light harvesting efficiency (LHE) is defined as the fraction of incident light intensity (I_0) absorbed by the dye in the DSSCs[24,25]:

$$\text{LHE}=A=I_A/I_0 \quad (1)$$

where A is absorptance and I_A is the absorbed light intensity. By assuming the quantum yield of charge injection and charge collection of the cells to be constant throughout our study, the ΔJ_{sc} can be calculated by the following equation[25],

$$\Delta Jsc = \frac{\int[LHE_{pc}(\lambda)]F(\lambda)d\lambda - \int[LHE_{ref}(\lambda)]F(\lambda)d\lambda}{\int[LHE_{ref}(\lambda)]F(\lambda)d\lambda} \quad (2)$$

where $F(\lambda)$ is the photon flux as a function of wavelength λ, which is calculated from the standard AM 1.5G solar spectral irradiance[26].

3. Results and discussion

3.1 Microstructure and optical properties of TiO_2 NTPC coupled photoanodes

Fig. 1a displays the scheme of the hierarchical DSSC presented in this work, where a highly reflective TiO_2 NTPC was built onto the active TiO_2 NP layer. The TiO_2 NTPC as shown in Fig. 1b has been demonstrated to be able to significantly increase the photocurrent of the device through both PC and scattering effects[23]. The lattice constant of all TiO_2 NTPCs used in this study was fixed to ~150nm, an optimized value for the hetero-structured photoanodes due to the suitable Bragg position of the

NTPC. To further optimize the PCE of the TiO_2 NTPC coupled DSSCs and to explore the effect of TiO_2 NTPC on thin NP electrode, various thickness values of the TiO_2 NTPC and NP layers were studied (2.3, 4.5, 6.7 and 9μm for NTPC layer and 3, 5 and 10μm for NP layer). The cross-sectional images of four typical photoanodes are shown in Fig. 1c-f.

Fig. 2 shows the reflectance spectra of the photoanode coupled with TiO_2 NTPC (lattice constant of 150nm) measured under normal incidence in air and ethanol, whose refractive index is close to the 3-methoxy propionitrile based electrolyte used in the device. The absorption curve of N719 dye solution is also plotted for comparison. It can be seen that the stop band position of the TiO_2 NTPC used in this study is located at ~450nm in air, resulting a purple color of the PC coupled membrane, as shown in the inset of Fig. 2. The membranes remain an interesting semi-transparency, although they become less transparent as the thickness increases, in agreement with the transmission spectra of the photoanodes (Fig. S1). After being infiltrated with ethanol, the TiO_2 NPPC shows a reflectance peak that highly overlaps with the ruthenium dye absorption peak, a key to achieving the greatest photocurrent efficiency enhancement for the integrated DSSCs.

3.2 Performances of TiO_2 NTPC coupled thin and semi-transparent electrodes

In order to optimize the architecture of the NTPC coupled DSSCs and to evaluate the coupling effect on thin and semi-transparent nc-TiO_2 electrodes, for which the enhancement effect is expected to be large[27], photocurrent-voltage (*J-V*) curves were measured on DSSCs with NTPC and NP layers in different thickness, as shown

in Fig. 3. The photovoltaic parameters of these cells are also summarized in Table 1. Two interesting phenomena are readily observable from Fig. 3 and 4. One is that, in general, the coupling of the NTPC enhances the photocurrent and the efficiency. For thin and semi-transparent NP layers (l_{np}~3 and 5μm), the photocurrent generally increases with increasing thickness of the NTPC layer, an expected result due to a stronger PC effect and more dye loading in thicker NTPC layer[23]. For a thick NP layer (l_{np}~10μm), the optimum thickness for the NTPC layer is l_{np}~4.5μm (Fig. 3d). Further increasing the thickness of the TiO_2 NTPC layer to 6.7 and 9 μm will deteriorate the cell performance, due to the experimentally observed decrease in dye loading amount (Table 1) and the deteriorated charge transport and recombination in a very thick photoanode[28,29]. The maximum PCE of 7.1% was obtained in the 10μm NP+30c NTPC cell, which was 51.7% higher than that of the 10μm NP reference cell. This enhancement effect can be attributed to the multifunction of the TiO_2 NTPC layer, acting as a highly reflective Bragg mirror and a dye absorbing layer, which also harvests light[23]. At the same time, the Fabry-Perot cavity behavior of NTPC leads to increased light harvesting at the two band edges[11,30], which can be observed in this study by comparing the simulated absorptance spectra of DSSCs based on 15c NTPC and 60c NTPC, as the absorption increases in the extended spectral range (Fig. 4a and b). The experimental IPCE results are shown in Fig. 4c and the simulated absorptance spectra of DSSCs based on 30c NTPC and 45c NTPC are plotted in Fig. S2.

The other interesting thing is that in addition to the noticeable increase in short circuit current (J_{sc}) for all the devices coupled to the NTPC layer, the percentage photocurrent enhancement is more pronounced for thin and semi-transparent NP layer (Fig. 3d), because the ratio between the unabsorbed photons reflected back from the NTPC layer and the absorbed ones is greater in thinner NP layer. Assuming the absorptance of the NP layer to be A and the reflectance of the NTPC layer to be R, a simple estimation (neglecting the contribution from the NTPC) shows that the percentage increase in photocurrent is $(1\text{-}A)R$, which increases as the NP layer is thinner (or as A is smaller). If the additional light harvesting from the NTPC layer is counted, an even higher percentage increased (higher than 100%) in photocurrent can be obtained. Consequently, the photocurrent enhancement is within 58.4%~69.6% and 86.4%~126.2% for ~5-μm-thick and ~3-μm-thick NP electrode, respectively, after been coupled by the TiO_2 NTPC layer. The theoretically calculated photocurrent enhancement (Fig. 4d) verifies this thickness dependence. The experimental results generally follow this theoretically predicted trend, with slight discrepancies aroused from the fact that our theoretical calculation (Equations 1 and 2) neglected the influence of the NTPC electrode on the dye absorption amount and the charge transport. As a result of the multi-functionalities of the NTPC, a remarkable photocurrent enhancement of 126.2% was obtained in the 3μm NP+45c NTPC cell, with a PCE ~5.35%. As transparency is an attractive feature to be considered for DSSC, in our case, the most transparent cell, 3μm NP+15c NTPC, shows an efficiency of 4.66%, 99.1% higher than that of the reference 3μm NP cell.

In general, the open circuit voltage (V_{oc}) in a TiO_2 NT based cell is slightly higher than that in a TiO_2 NP based one due to the superior charge transport characteristics of the NT to that of the NP[28]. Hence for thin NP layers (l_{np}~3 and 5μm), the cells coupled with the NTPC layer generally show higher V_{oc}, except the 3μm NP+60c NTPC cell. However, when the photoanodes become too thick, no matter for the thick NP layer (l_{np}~10μm) or the thick NTPC layer (60c NTPC), the V_{oc} of the cell starts to decrease, due to the deteriated charge recombination kinetics. Similar phenomena have also been observed in our and Colodrero′s work[22,27,31]. The observed variation of V_{oc} is a competition of effects due to the NTPC layer and the overall thickness of the photoanode.

3.3 Performances of TiO_2 NTPC coupled thin and semi-transparent electrodes working under low photon flux conditions

It is well-known that under oblique illumination, the intensity of light I decreases with the incident angle θ, following a cosine law, $I=I_0\cos\theta$, which causes an inevitable output energy loss for solar cells operating under tilted sunlight[15,32]. Fig. 5 shows the angular dependence of the *J-V* curves of integrated DSSCs with different TiO_2 NP and NTPC layer thicknesses. It can be seen that, in general, the J_{sc} of all the cells decreases with increasing incident angle as a result of the cosine loss in light intensity. However, by comparing the left column in Fig. 5 with the right one, it is found that the decrease in J_{sc} as a result of tilted incident angle can be made less significant by coupling to a thicker NTPC layer, particularly for thicker NP electrode. For comparison, the *J-V* curves of TiO_2 NP based reference cells with different

thickness are presented in Fig. S3.

A detailed analysis of the evolution of J_{sc} with the incident angle is displayed in Fig. 6. It can be seen that for all the reference NP cells, the drop in J_{sc} observed experimentally shows a thickness dependence not exactly following the cosine of incident angle since the optical path in the photoanode becomes longer when the light is tilted[15]. After the TiO_2 NTPC is integrated to the DSSCs, the angular dependence of the photocurrent becomes more flattened, a desired feature for a stable power output under oblique incidence. This decrease of the angular dependence of the photocurrent is a consequence of the additional scattering effect of the TiO_2 nanotube walls when the incident light is at an angle to the axial direction of the nanotubes, indicating the compensation effect of TiO_2 NTPC to the energy loss of DSSCs under inclined incidence. It should be noted that under oblique incidence, the Bragg position of the PC structure blue shifts[33], as shown in the simulated angular evolution of absorbance spectra of NTPC coupled DSSCs (Fig. S4a and b). In a separate work, we have shown that this blue shift of the Bragg position of the NTPC under oblique light can be utilized to design a NTPC coupled DSSC with an even smaller angular dependence of the photovoltaic performance[34]. It is also noted that the compensation effect due to the scattering of the nanotube structure becomes more significant for thinner NP electrode, as theoretically predicted in Fig. S4c and d, leading to smaller angular dependence of the photocurrent. The experimental results shown in Fig. 6c and d agree well with the theoretical calculation. This compensation effect and its variation with the thickness of the NP electrode can be clearly seen in

Fig. 6e and f, in which the J_{sc} enhancement increases with the incident angle, and this increasing trend becomes steeper for thinner NP layer, compensating the cosine energy loss as the incident light is tilted. Consequently, the PCE shows similar evolution to that of J_{sc}, as shown in Fig. S5a-d (with the angular response of V_{oc} and *FF* plotted in Fig. S5c and d).

Finally, the performances of the TiO_2 NTPC coupled thin and semi-transparent DSSCs working under different light intensity were studied since, in certain real applications, DSSCs are preferred to be used in low irradiance conditions. The *J-V* characteristics of a ~3-μm-thick TiO_2 NP electrode coupled with the 15c NTPC measured under different light intensity of 50, 75, 100 and 125mW·cm^{-2} are displayed in Fig. 7a, and that of the reference cells with the same NP layer thickness are also plotted for comparison in Fig. 7b. It can be seen that the introduction of the NTPC layer leads to a significant photocurrent increase under all illumination intensity tested. Combined with the decreased V_{oc} and the oppositely increased *FF* as the light intensity declines (Fig. 7c), which are resulted from lower density of carriers, giving rise to better electron transport and recombination[35], the thin and semi-transparent DSSCs coupled with the 15c NTPC shows a PCE of 5.03% under the intensity of 50mW·cm^{-2}, 130% higher than that of the reference cell, as shown in Fig. 7d.

4. Conclusions

We have shown that the photovoltaic performances of thin and semi-transparent nc-TiO_2 DSSCs can be significantly enhanced by coupling the NP electrode with the TiO_2 NTPC layer, due to the multi-functionalities provided by the NTPC structure,

such as, Bragg reflection, random scatting, and additional light harvesting from the TiO_2 nanotubes. Compared with the 3-μm-thick TiO_2 NP based reference DSSCs, the PCE is enhanced by 99.1% when a 2.3-μm-thick TiO_2 NTPC is coupled, and this value is further increased up to 130% under 0.5 Sun condition. Under tilted illumination, the NTPC coupled DSSCs show smaller angular dependence of the photocurrent, due to the compensation effect provided by the light scattering from the walls of nanotubes. These results demonstrate that the TiO_2 NTPC structure is particularly suitable for thin and semi-transparent DSSCs under normal, titled or low irradiance illumination conditions, very much desired for practical applications.

Acknowledgements

This work was supported by the Research Grants Council of the Hong Kong Special Administrative Region (Project Nos. PolyU152057/14E and PolyU5163/12E). The authors also appreciate the financial supports from the National Natural Science Foundation of China (No.51302219), the Fundamental Research Funds for the Central Universities (No. 3102014JCQ01019), and the Research Fund of the State Key Laboratory of Solidification Processing (NWPU), China (Grant No.83-TZ-2013).

Appendix A. Supplementary data

Supplementary data related to this article can be found at http://

References

[1] J. Halme, P. Vahermaa, K. Miettunen, P. Lund, Adv. Mater. 22(2010) E210-E234.

[2] K. A. Arpin, A. Mihi, H. T. Johnson, A. J. Baca, J. A. Rogers, J. A. Lewis, P. V. Braun, Adv. Mater. 22(2010)1084-1101.

[3] S. Pillai, K. R. Catchpole, T. Trupke, M. A. Green, J. Appl. Phys. 101(2007)8.

[4] A. Yella, H.-W. Lee, H. N. Tsao, C. Yi, A. K. Chandiran, M. K. Nazeeruddin, E. W.-G. Diau, C.-Y. Yeh, S. M. Zakeeruddin, M. Grätzel, Science 334(2011)629-634.

[5] M. Fujita, S. Takahashi, Y. Tanaka, T. Asano, S. Noda, Science 308(2005)1296-1298.

[6] L. Peres, V. Vigneras, S. Fasquel, Sol. Energ. Mat. Sol. C. 117(2013)239-245.

[7] S. Bayram, L. Halaoui, Part. Part. Syst. Charact. 30(2013)706-714.

[8] M. El Harakeh, L. Halaoui, J. Phys. Chem. C 114(2010)2806-2813.

[9] J. Upping, A. Bielawny, R. B. Wehrspohn, T. Beckers, R. Carius, U. Rau, S. Fahr, C. Rockstuhl, F. Lederer, M. Kroll, T. Pertsch, L. Steidl, R. Zentel, Adv. Mater. 23(2011)3896-3900.

[10] D. Colonna, S. Colodrero, H. Lindstrom, A. Di Carlo, H. Miguez, Energy Environ. Sci. 5(2012)8238-8243.

[11] M. Guo, Z. H. Yong, K. Y. Xie, J. Lin, Y. Wang, H. T. Huang, ACS Appl. Mater Inter. 5(2013)13022-13028.

[12] M. E. Calvo, S. Colodrero, N. Hidalgo, G. Lozano, C. Lopez-Lopez, O. Sanchez-Sobrado, H. Miguez, Energy Environ. Sci. 4(2011)4800-4812.

[13] D. H. Ko, J. R. Tumbleston, L. Zhang, S. Williams, J. M. DeSimone, R. Lopez, E. T. Samulski, Nano Lett. 9(2009)2742-2746.

[14] S. John, Phys. Rev. Lett. 58(1987)2486-2489.

[15] C. Lopez-Lopez, S. Colodrero, M. E. Calvo, H. Miguez, Energy Environ. Sci. 6(2013)1260-1266.

[16] X. Sheng, L. Z. Broderick, L. C. Kimerling, Opt. Commun.314(2014)41-47.

[17] S. Nishimura, N. Abrams, B. A. Lewis, L. I. Halaoui, T. E. Mallouk, K. D. Benkstein, J. van de Lagemaat, A. J. Frank, J. Am. Chem. Soc. 125(2003)6306-6310.

[18] L. P. Heiniger, P. G. O'Brien, N. Soheilnia, Y. Yang, N. P. Kherani, M. Gratzel, G. A. Ozin, N. Tetreault, Adv. Mater. 25(2013)5734-5741.

[19] J. T. Park, J. H. Prosser, D. J. Kim, J. H. Kim, D. Lee, ChemSusChem 6(2013)856-864.

[20] D. Colonna, S. Colodrero, H. Lindstrom, A. Di Carlo, H. Míguez, Energy Environ. Sci. 5(2012)8238-8243.

[21] J. T. Park, J. H. Prosser, S. H. Ahn, S. J. Kim, J. H. Kim, D. Lee, Adv. Funct. Mater. 23(2012)2193-2200.

[22] C. T. Yip, H. Huang, L. Zhou, K. Xie, Y. Wang, T. Feng, J. Li, W. Y. Tam, Adv. Mater. 23(2011)5624-5628.

[23] M. Guo, K. Xie, J. Lin, Z. Yong, C. T. Yip, L. Zhou, Y. Wang, H. Huang, Energy Environ. Sci., 5(2012)9881-9888.

[24] A. Mihi, H. Míguez, J. Phys. Chem. B 109(2005)15968-15976.

[25] A. Mihi, F. J. López-Alcaraz, H. Míguez, Appl. Phys. Lett. 88(2006)193110.

[26] Standard spectrum taken from http://www.nrel.gov/r-redc/.

[27] S. Colodrero, A. Forneli, C. López-López, L. Pellejà, H. Míguez, E. Palomares, Adv. Funct. Mater. 22(2012)1303-1310.

[28] Q. Zheng, H. Kang, J. Yun, J. Lee, J. H. Park, S. Baik, ACS Nano 5(2011)5088-5093.

[29] L. Cao, C. Wu, Q. Hu, T. Jin, B. Chi, J. Pu, L. Jian, G. Rohrer, J. Am. Ceram. Soc. 96(2012)549-554.

[30] O. N. Kozina, L. A. Mel'nikov, Laser Phys. 14(2004)727-732.

[31] S. Ito, S. M. Zakeeruddin, R. Humphry-Baker, P. Liska, R. Charvet, P. Comte, M. K. Nazeeruddin, P. Pechy, M. Takata, H. Miura, S. Uchida, M. Gratzel, Adv. Mater. 18(2006)1202-1205.

[32] J. D. Joannopoulos, P. R. Villeneuve, S. H. Fan, Nature 386(1997)143-149.

[33] L. Liu, S. K. Karuturi, L. T. Su, A. I. Y. Tok, Energy Environ. Sci. 4(2011)209-215.

[34] M. Guo, K. Xie, X. Liu, Y. Wang, L. Zhou, H. Huang, Nanoscale 6(2014)13060-13067.

[35] S. Colodrero, A. Mihi, L. Häggman, M. Ocaña, G. Boschloo, A. Hagfeldt, H. Míguez, Adv. Mater. 21(2009)764-770.

Captions

Fig. 1 Design and microstructure of a DSSC coupled with a TiO_2 NTPC layer. (a) Scheme of the solar cell consisting of TiO_2 NP and NTPC layers of thicknesses l_{np} and l_{pc}, respectively. (b) Microstructure of TiO_2 NTPC with lattice constant of 150nm. The scale bar measures 100nm. (c-f) Cross-sectional FESEM images of TiO_2 NTPC/NP electrodes with different thicknesses: (c) l_{np}=~3μm, l_{pc}=~2.3μm; (d) l_{np}=~10μm, l_{pc}=~2.3μm; (e) l_{np}=~3μm, l_{pc}=~9μm; and (f) l_{np}=~10μm, l_{pc}=~9μm. The scale bars measure 1μm.

Fig. 2 Reflectance spectra of TiO_2 NTPC (lattice constant of 150nm) coupled photoanode under normal incidence in air and ethanol. The thicknesses of the NTPC and NP layers are l_{np}~10μm and l_{pc}~2.3μm. The absorption of N719 dye is also plotted as black dashed line. The insets are photos of the photoanodes of l_{np}~3μm, l_{pc}~2.3μm (top) and l_{np}~10μm, l_{pc}~9μm (bottom).

Fig. 3 Photocurrent-voltage curves of DSSCs with TiO_2 NTPC and NP layers in different thickness: (a) l_{np} ~3μm, (b) l_{np} ~5 μm,and (c) l_{np} ~ 10μm. The black line in each graph is the J-V curve of a reference cell with only the TiO_2 NP electrode which has the same thickness l_{np}. (d) Electrode thickness dependence of the photocurrent enhancement (as compared to the photocurrent of the TiO_2 NP reference electrode) due to the coupling of TiO_2 NTPC layer. The *x*-axis refers to the thickness of the NP layer.

Fig. 4 (a-b) Numerically simulated absorptance curves and (c) experimental IPCEs of the DSSCs coupled with different TiO_2 NTPCs. The curves of a reference DSSC based on the NP electrode only are also shown for comparison. (d) The calculated photocurrent enhancement (as compared to the photocurrent of the TiO_2 NP reference electrode) due to the coupling of different TiO_2 NTPC layers.

Fig. 5 The photocurrent-voltage curves of TiO_2 NTPC coupled DSSCs with different TiO_2 NP layer thicknesses, (a-b) 3μm, (c-d) 5μm and (e-f) 10μm, measured under different incident angles from 0° and 60°, in a step of 5°. The left and right columns are cells coupled with 15c NTPC and 60c NTPC, respectively.

Fig. 6 Angular dependence of (a, b) J_{sc}, (c, d) normalized J_{sc} and cosine curve, and (e, f) J_{sc} enhancement (as compared to the corresponding reference cell) for DSSCs coupled with 15c NTPC(left column) and 60c NTPC (right column). The corresponding NP layer thickness is ~3μm (red line), 5μm (green line) and 10μm (blue line). For comparison, the curves for the reference NP cells are also shown, ~3μm (grey line), 5μm (dark grey line) and 10μm (black dashed line).

Fig. 7 The photocurrent-voltage curves of (a) 15c NTPC coupled thin and semi-transparent DSSC (~3μm thick NP layer) and (b) reference DSSC with the NP layer of the same thickness, operating under different irradiances of 50, 75, 100 and 125 $mW \cdot cm^{-2}$. (c) V_{oc} and FF, (d) J_{sc} and η evolution of these cells under different light intensities.

Table 1. Characteristic photovoltaic parameters of the samples

Table 1. Characteristic photovoltaic parameters of the samples

Photoanode	V_{oc}	J_{sc}	FF	η	ΔJ_{sc}	$\Delta\eta$	Thickness	Dye loading
~3μm NP	0.731	5.30	60.4	2.34	--	--	~3.0	43.14
~3μm NP+15c NTPC	0.759	9.88	62.1	4.66	86.4	99.1	~5.3	64.50
~3μm NP +30c NTPC	0.747	10.91	61.1	4.97	105.8	112.4	~7.5	77.19
~3μm NP +45c NTPC	0.746	11.99	59.8	5.35	126.2	128.6	~9.7	90.45
~3μm NP +60c NTPC	0.739	11.41	59.9	5.05	115.3	115.8	~12.0	94.47
~5μm NP	0.718	8.56	59.6	3.66	--	--	~5.0	69.38
~5μm NP +15c NTPC	0.736	13.56	61.4	6.12	58.4	67.2	~7.3	82.71
~5μm NP +30c NTPC	0.734	13.70	60.7	6.10	60.0	66.7	~9.5	97.95
~5μm NP +45c NTPC	0.721	14.13	60.3	6.15	65.1	68.0	~11.7	108.60
~5μm NP +60c NTPC	0.706	14.52	60.8	6.23	69.6	70.2	~14.0	105.59
~10μm NP	0.706	11.09	59.8	4.68	--	--	~10.0	110.15
~10μm NP +15c NTPC	0.705	15.57	61.8	6.78	40.4	44.9	~12.3	130.75
~10μm NP +30c NTPC	0.706	16.10	62.5	7.10	45.2	51.7	~14.5	147.68
~10μm NP +45c NTPC	0.697	14.69	60.4	6.19	32.5	32.3	~16.7	145.06
~10μm NP +60c NTPC	0.693	13.22	61.3	5.62	19.2	20.1	~19.0	125.53

V_{oc}: Open circuit voltage (V), J_{sc}: Short circuit current (mA·cm^{-2}), FF: Fill factor (%), η: Power conversion efficiency (%), $\Delta J_{sc}/J_{sc}$: Percentage enhancement in J_{sc} (%), $\Delta\eta/\eta$: Percentage enhancement in η (%), Thickness: (μm), Dye loading: (nmol·cm^{-2}).

Figure 1

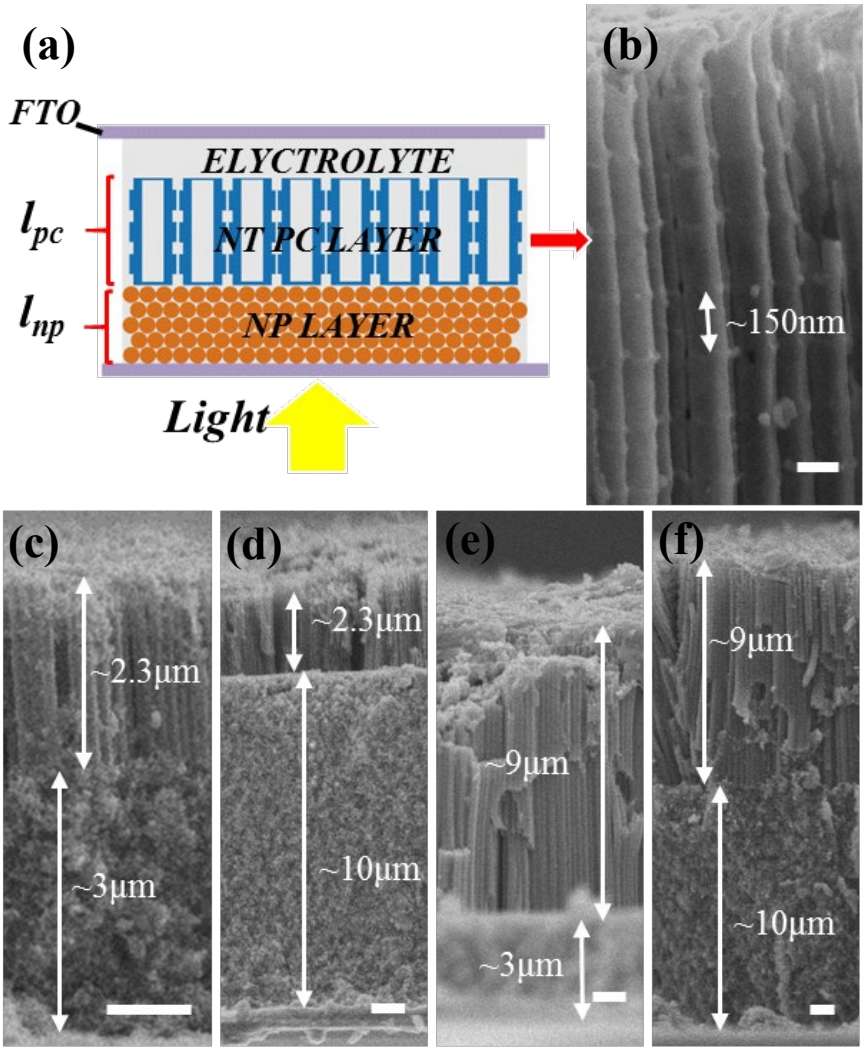

Fig. 1 Design and microstructure of a DSSC coupled with a TiO_2 NTPC layer. (a) Scheme of the solar cell consisting of TiO_2 NP and NTPC layers of thicknesses l_{np} and l_{pc}, respectively. (b) Microstructure of TiO_2 NTPC with lattice constant of 150nm. The scale bar measures 100nm. (c-f) Cross-sectional FESEM images of TiO_2 NTPC/NP electrodes with different thicknesses: (c) l_{np}=~3μm, l_{pc}=~2.3μm; (d) l_{np}=~10μm, l_{pc}=~2.3μm; (e) l_{np}=~3μm, l_{pc}=~9μm; and (f) l_{np}=~10μm, l_{pc}=~9μm. The scale bars measure 1μm.

Figure 2

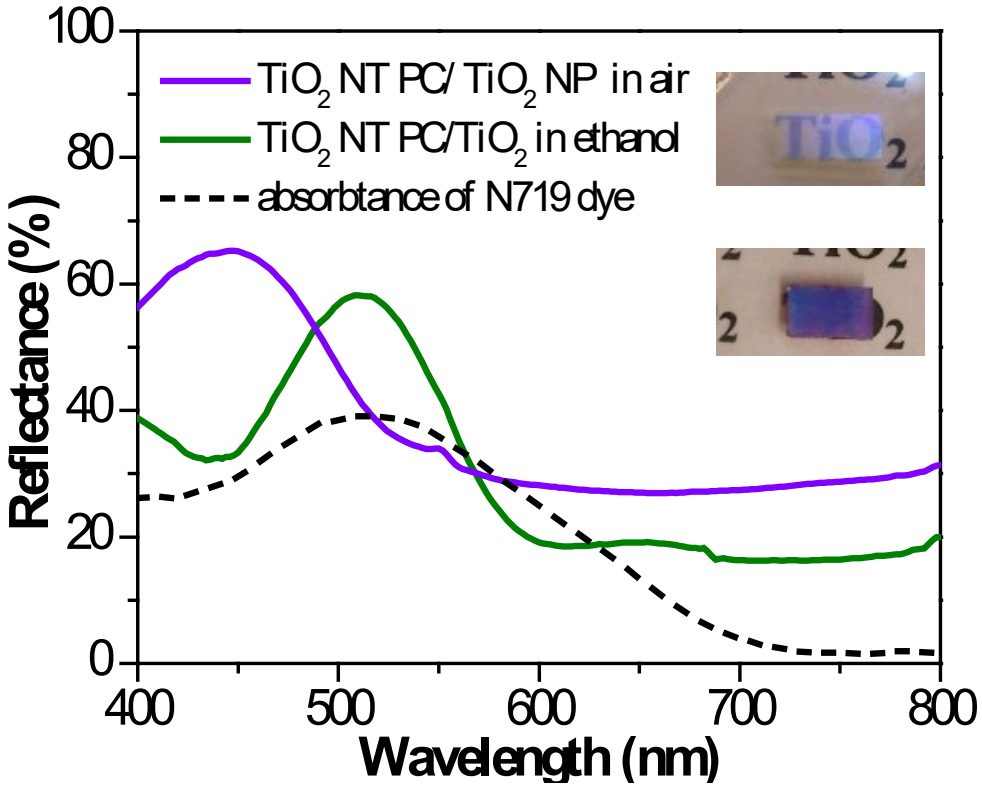

Fig. 2 Reflectance spectra of TiO_2 NTPC (lattice constant of 150nm) coupled photoanode under normal incidence in air and ethanol. The thicknesses of the NTPC and NP layers are l_{np}~10μm and l_{pc}~2.3μm. The absorption of N719 dye is also plotted as black dashed line. The insets are photos of the photoanodes of l_{np}~3μm, l_{pc}~2.3μm (top) and l_{np}~10μm, l_{pc}~9μm (bottom).

Figure 3

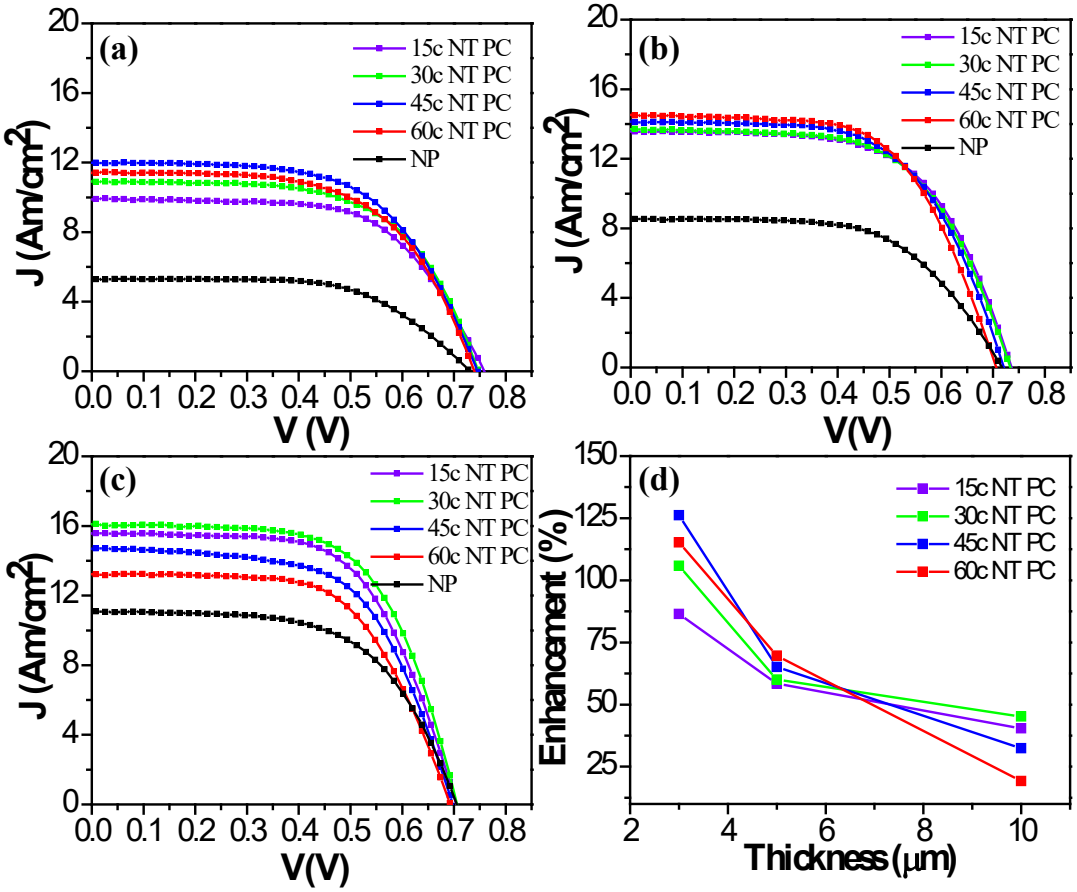

Fig. 3 Photocurrent-voltage curves of DSSCs with TiO_2 NTPC and NP layers in different thickness: (a) l_{np} ~3μm, (b) l_{np} ~5 μm,and (c) l_{np} ~ 10μm. The black line in each graph is the J-V curve of a reference cell with only the TiO_2 NP electrode which has the same thickness l_{np}. (d) Electrode thickness dependence of the photocurrent enhancement (as compared to the photocurrent of the TiO_2 NP reference electrode) due to the coupling of TiO_2 NTPC layer. The *x*-axis refers to the thickness of the NP layer.

Figure 4

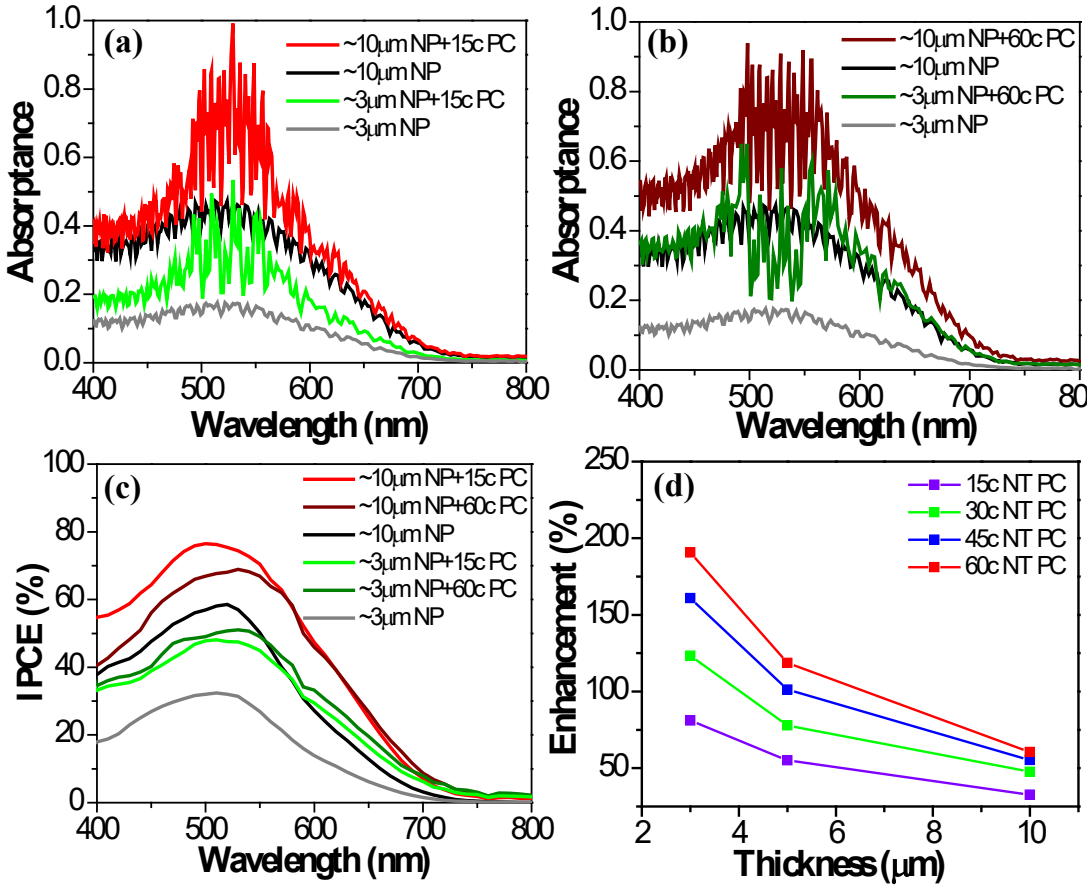

Fig. 4 (a-b) Numerically simulated absorptance curves and (c) experimental IPCEs of the DSSCs coupled with different TiO_2 NTPCs. The curves of a reference DSSC based on the NP electrode only are also shown for comparison. (d) The calculated photocurrent enhancement (as compared to the photocurrent of the TiO_2 NP reference electrode) due to the coupling of different TiO_2 NTPC layers.

Figure 5

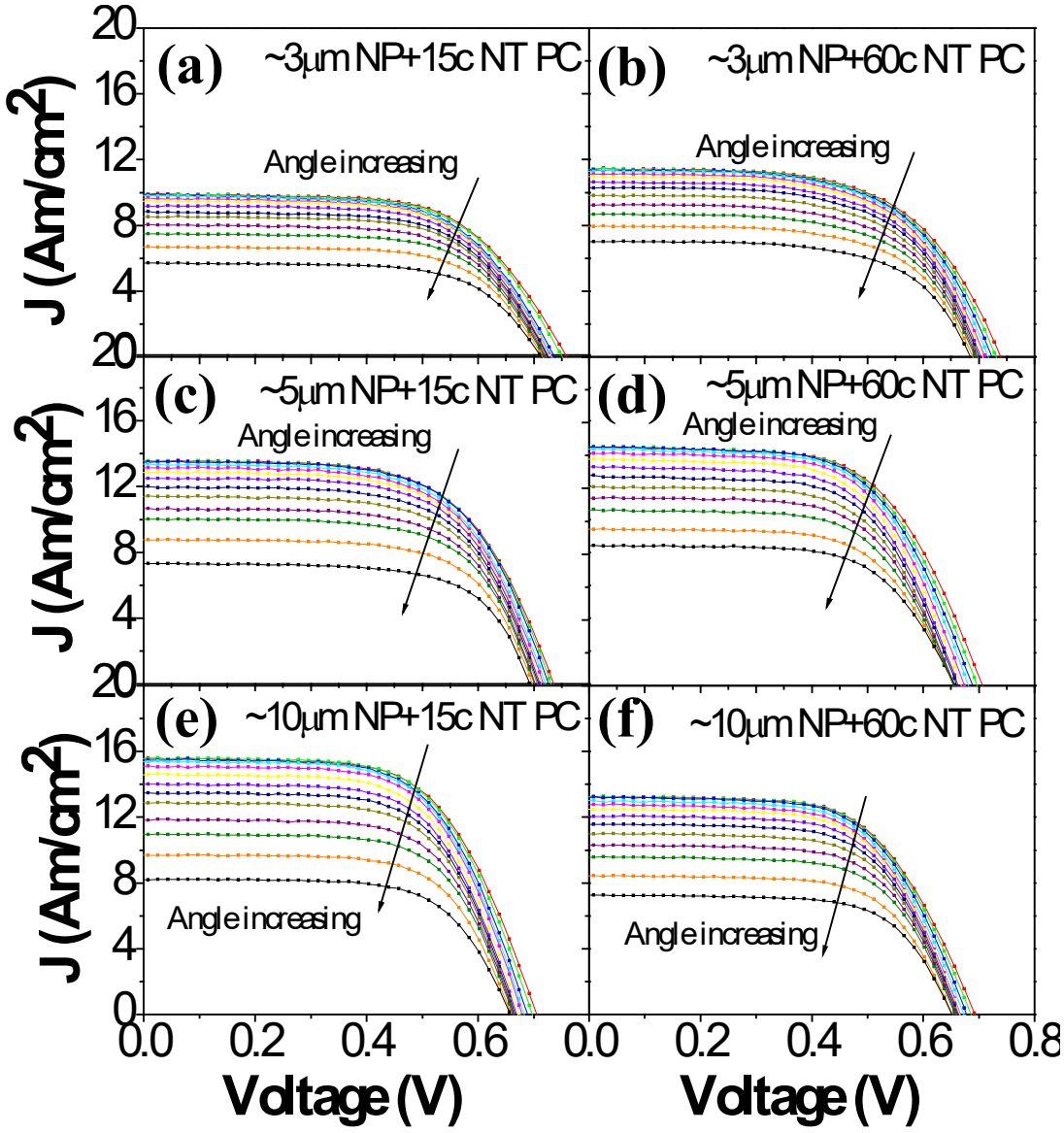

Fig. 5 The photocurrent-voltage curves of TiO_2 NTPC coupled DSSCs with different TiO_2 NP layer thicknesses, (a-b) 3μm, (c-d) 5μm and (e-f) 10μm, measured under different incident angles from 0° and 60°, in a step of 5°. The left and right columns are cells coupled with 15c NTPC and 60c NTPC, respectively.

Figure 6

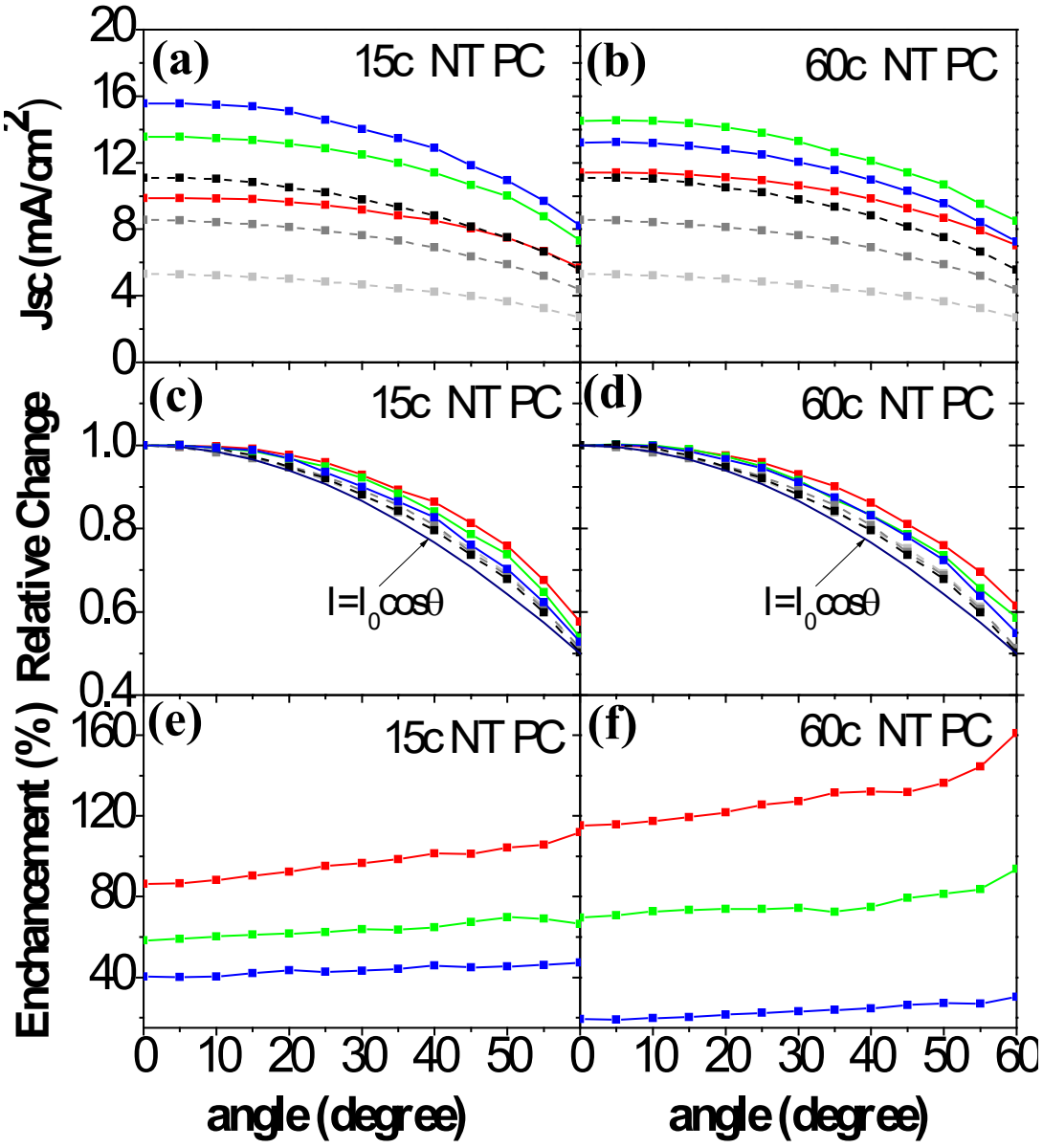

Fig. 6 Angular dependence of (a, b) J_{sc}, (c, d) normalized J_{sc} and cosine curve, and (e, f) J_{sc} enhancement (as compared to the corresponding reference cell) for DSSCs coupled with 15c NTPC (left column) and 60c NTPC (right column). The corresponding NP layer thickness is ~3μm (red line), 5μm (green line) and 10μm (blue line). For comparison, the curves for the reference NP cells are also shown, ~3μm (grey line), 5μm (dark grey line) and 10μm (black dashed line).

Figure 7

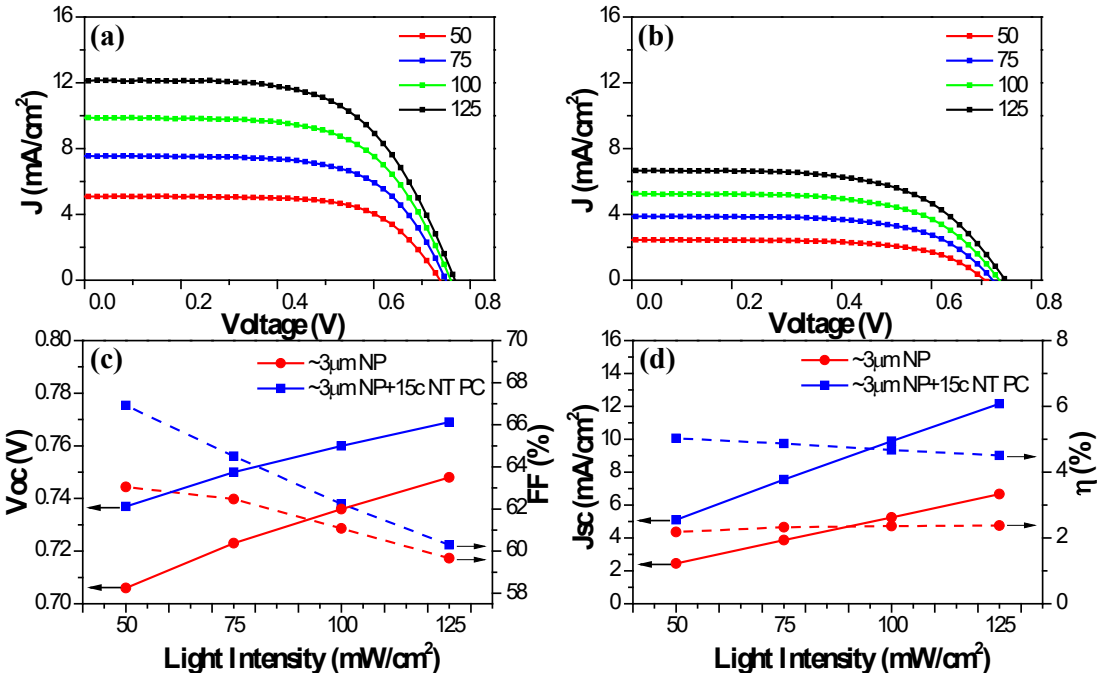

Fig. 7 The photocurrent-voltage curves of (a) 15c NTPC coupled thin and semi-transparent DSSC (~3μm thick NP layer) and (b) reference DSSC with the NP layer of the same thickness, operating under different irradiances of 50, 75, 100 and 125 mW·cm^{-2}. (c) V_{oc} and *FF*, (d) J_{sc} and η evolution of these cells under different light intensities.